Monomer Distribution Functions of a Ternary Polymer System: A Monte Carlo Investigation

A. Sariban[†]

Institut für Physik, Johannes Gutenberg Universität Mainz, D-6500 Mainz, Postfach 3980, Federal Republic of Germany

Received January 18, 1990; Revised Manuscript Received July 19, 1990

ABSTRACT: A ternary system, consisting of 40% macromolecules of species A, one macromolecule of species B, and vacancies (low molecular solvent), is modeled by the Monte Carlo simulation on a classical Flory–Huggins lattice. The polymers are represented by self-avoiding walks. The number of links in a lattice chain is chosen as $N_A = N_B = N$, with $N = 16$, 32, and 64. Nearest-neighbor interaction is assumed to be $\epsilon_{AA} = \epsilon_{BB} = \epsilon$. $\epsilon_{AB} = 0$ where ϵ is varied from good-solvent condition to collapse transition condition for B. The monomer distribution functions of A and B species around the center of inertia of A and B molecules are obtained as well as the distribution function of a given A,B chain around its own center of inertia. The latter functions are of Gaussian type for both A and B

$$P(r) = \frac{N}{R_g^{\,3}}\alpha \exp\left(-\frac{3}{2}\frac{r^2}{R_g^{\,2}}\right) \tag{1}$$

for all N and ϵ (where R_g is the radius of inertia of the chain) and $\alpha \sim 0.37$. From the distribution of A monomers around the A chain, two regions are found: (a) Monomer A and vacancies tend to separate for large ϵ. (b) The polymer A–solvent system is macroscopically homogeneous but has local inhomogeneities—the density of monomers A in the vicinity of the center of gravity of A is larger than the mean polymer concentration in solution. We try to describe this effect by an "improved quasi-binary approximation". The distribution function of A monomers around a single B chain under "strictly" homogeneous conditions seems to obey the law

$$P_{AaB}(r) = F(r{\cdot}R_{Bg}^{\,2}) \tag{2}$$

(R_{Bg} is the radius of inertia of the chain B.)

1. Introduction

In this work computer calculations are performed on a model system consisting of one molecule of one polymer species ("guest"), 40% volume of another species of polymer ("host"), and the remaining volume consisting of vacancies (modeling low molecular solvent). This work has two aims: (1) to study the behavior of one (guest) molecule in a mixed solvent consisting of polymer and a low molecular species; (2) to study the semidilute polymer solution consisting of host molecules (note that one guest molecule should not influence the behavior of the host polymer–solvent system appreciably). The main aim of this work is to establish the distribution of monomers of different species around the center of gravity of the guest or host polymer.

The question as to how macromolecules of very low concentration behave in a poor solvent (so-called "coil–globule transition") is the topic of a lot of research work. The coil–globule transition is important in connection with problems in biophysics concerning the denaturation of peptides.[1] However, it is also related to "normal" (mostly synthetic) polymers. In the latter case, the specific forces that play an important role in the formation of secondary and ternary structures in biological molecules are not relevant (see ref 2, where some important experimental observations and relevant theoretical models are discussed and later experimental works[3]). One of the main problems here concerns the statistical mechanical law, which the coil–globule transition obeys. de Gennes[4] has discussed the analogy between the coil–globule transition at the θ point and tricritical behavior. Moore[5] showed that the coil–globule phase transition occurs at the θ temperature in the infinite N limit (where N is the degree of polymerization of the macromolecule) and that the transition is of second order. He criticized the results obtained by Lifshitz,[6] who obtained both first- and second-order transitions under various circumstances. Post and Zimm,[7] by using a virial expansion in the Flory theory and evaluating the third virial coefficient, found that a critical point occurs for suitable thermodynamic polymer flexibility. If the flexibility is lower than a critical value, there is a first-order phase transition from expanded coil to globule. The flexible macromolecule expands and contracts in a continuous fashion. This result agrees with the old numerical results of Elyashevich and Skvortsov.[8] Using Monte Carlo simulations, they observed a first-order coil–globule phase transition for semiflexible macromolecules and continuous collapse from the coil to the globule by making solvent poorer for flexible macromolecules. The coil–globule transition in low molecular solutions can be treated using the "thermal-blob model",[9] where the single chain is described as a succession of Gaussian blobs, each consisting of N_τ segments, with excluded-volume interaction between the blobs (τ is a solvent goodness parameter; N_τ is a cutoff value separating Gaussian and excluded-volume regions, where N_τ is defined by $|\tau|{\cdot}N_\tau^{1/2} = 1$). Different theoretical approaches predict the asymptotical law $R_g \sim N^{1/3}|\tau|^{-1/3}$[2] for the radius of gyration (R_g) of flexible chains in the pure solvent.

The behavior of a dilute polymer chain in a mixed solvent of another polymer species and a low molecular weight substance has excited considerable interest in the past 10 years. Lerman[10] observed condensation of viral DNA of high molecular weight (approximately 10^7) in aqueous salt solution of poly(ethylene oxide) with a molecular weight

---

[†] Present address: Technische Hochschule Darmstadt, Physikalische Chemie, Petersenstrasse 20, D-6100 Darmstadt, FRG.

0024-9297/91/2224-1134$02.50/0 © 1991 American Chemical Society

of about 7000. This work was an impetus for theoretical[7,11,12] and experimental[14] investigations, using the macromolecule as the guest in mixed solutions and smaller host macromolecules.

Nose[15] presented a theory where the chain dimension of a guest in a semidilute solution of compatible and incompatible polymers was treated (without the rigorous restriction $N_{\text{guest}} \gg N_{\text{host}}$). In his treatment the effective excluded-volume parameter τ is a function of guest–host interaction χ, host-concentration ϕ, and the length of the host chain. For $\chi = 0$ his results coincided with those of Joanny et al.,[16] who treated a binodal mixture of chemically identical polymers in a good solvent.

Here we also mention some experimental work, treating a ternary system of one dilute polymer species, one semidilute polymer species, and a low molecular weight solvent,[17-20] where the radius of gyration and the second virial coefficient of the guest molecule was measured.

The main interest of the present work lies in the study of the shape of the macromolecules, i.e., the density distribution function between monomers. There are various ideas regarding this function. The classical model, primarily based on conformational statistics of an ideal random, self-intersecting chain,[21] predicts the following distribution function between two monomers of one chain

$$W(r) = \left(\frac{3}{2\pi\langle r^2\rangle}\right)^{3/2} \exp\left(-\frac{3}{2}\frac{r^2}{\langle r^2\rangle}\right) \qquad (3)$$

where r is the distance between the monomers. This function, the so-called "Gaussian approximation", is often presumed to describe the average of the segment density distribution of real (non-self-intersecting) macromolecular chains in their center of gravity coordinate system.

For macromolecules $\langle r^2\rangle$ in eq 3 has to be replaced by R_g, the "real" mean-square radius of gyration of the macromolecule (depending on the "goodness" of the solvent). Obviously, because the molecule consists of N monomers, the right-hand side of eq 3 for the whole monomer density distribution in a molecule has to be multiplied with N.

We now turn to the theoretical predictions about the pair correlation function between monomers in a chain.[22] Inside an ideal chain we have

$$g(r) \sim 1/r \qquad (4)$$

and for the chain in a good solvent

$$g(r) \sim r^{-4/3} \qquad (5)$$

The distribution of the end-to-end distances in a self-avoiding walk of N steps has to obey the asymptotical laws

$$\varphi_{\text{p}}(x) \sim x^{g} \qquad x \to 0 \qquad (6)$$

$$\varphi_{\text{p}}(x) \sim \exp(-x^{\delta}) \qquad x \to \infty \qquad (7)$$

where $x = r/R_{\text{F}}$. R_{F} is the root-mean-square value of end-to-end distance, $g = {}^1/_3$ for three dimensions, and $\delta = (1 - \nu)^{-1}$ ($\nu = 0.6$ for the good solvent; $\nu = 0.5$ for Θ solvent; $\nu = 0.33$ for bad solvent).[22]

Des Cloizeaux[23] considered the end-to-end distance distribution of polymer chains and obtained the following scaling law:

$$\varphi(r) \sim \frac{1}{r^d}\phi(rN^{-\nu}) \qquad (8)$$

(d is space dimension.)

Table I
Signs for Different ϵ on Figures 2–4, 7, and 9–11

△	$E = 0$	⍋	$E = 0.30$
+	$E = 0.06$	⋊	$E = 0.42$
×	$E = 0.12$	Z	$E = 0.60$
◇	$E = 0.18$		

In addition, there are qualitatively different pictures concerning possible forms of the density distribution versus distance from the center of the globule: (a) uniformly varying density, (b) density distribution with a smoothed boundary, and (c) density distribution with microstructure.[6]

It appears to be very difficult to differentiate between the various predictions about the shape of the macromolecule experimentally, both for the coil–globule transition and for macromolecules in semidilute solution. Therefore, computer simulation is a very powerful tool in order to make progress in the understanding of this topic.

We now briefly recall what is known about the general structures of semidilute polymer solutions. Investigations during the last 20 years have led to the establishment of the "concentration blob" picture,[22] assuming that in the semidilute polymer solution there is a characteristic correlation length, ξ, which depends on the concentration of the polymer, c, where $\xi(c) \sim c^{-3/4}$ (for $d = 3$). If the distance between monomers is smaller than ξ, each chain "feels" only itself and exhibits typical "good" behavior on this scale. For distances greater than ξ, the excluded-volume interaction is "screened" by other molecules and there is "ideal" behavior. The correlation length, ξ, does not depend on the length of macromolecule, N. However, the "semidilute solution" itself must have a polymer concentration larger than a characteristical value c^* where macromolecules begin to overlap

$$c^* \sim N^{-4/5} \qquad (9)$$

The other aspects of the polymer solution structure such as the pair correlation function between macromolecules have not been studied with such intensity. It is rather difficult to make progress here experimentally. We mention here the attempts to apply the Förster energy-transfer experiments to measure intermolecular correlation functions or similar characteristics of semidilute polymer solutions.[24,25]

There exist numerical calculations of the intermolecular pair distribution function in the melt, based on an integral equation approach.[26-28] However, this approach was specifically designed for undiluted polymers and cannot be applied to the semidilute regime considered in the present work.

There are several computer simulations in which the monomer distribution function of one molecule with respect to its center of mass[29-33] and pair distribution functions between monomers of different chains[31-35] were calculated.

In ref 36 and several other works the author determined the structure factor of one polymer chain (i.e., the Fourier transform of the density distribution function). In ref 37 the pair correlation function of the center of mass of macromolecules in a bulk was calculated by using the "reptation" Monte Carlo algorithm. However, much more work remains to be done.

The present paper has the following structure. In section 2 we describe the model and the method of calculation. In section 3 we discuss the behavior of the monomer distribution function of the host polymer. In section IV we show the density distribution function of monomers belonging to other chains with respect to the center of mass of a given chain of the host type. We try to describe this "intermolecular density distribution" of the binary polymer–low molecular weight solvent system by an empirical assumption, similar to the "quasi-binary approximation". In section 5 we deal with intramolecular characteristics of the chain of host and guest types. Our main interest lies in the intramolecular density distribution ("the shape") of the monomers. It was found that the shape of both host and guest macromolecules has a simple Gaussian form, similar to eq 3. In the section 6 we turn our attention to the behavior of the macromolecular environment, produced by host molecules around the center of mass of the guest molecule. It was found that if the guest–host solvent system does not show any tendency to phase separation, the host monomer environment against guest chain obeys a simple scaling law. Finally, in section 7 we summarize and discuss our main results.

2. Model and Calculation Method

The model used for the present calculation is described elsewhere:[38-40] Non-self-intersecting chains on a simple cubic lattice with interactions between nearest-neighbor segments. This corresponds to the classical Flory–Huggins model. The chains fill the box with periodic boundary conditions until the concentration 40%. Thus 60% of the lattice sites are vacancies when modeling low molecular weight solvents. The length of one side of the cubic box $L \times L \times L$ in lattice units is $L = 24$. One of the polymer chains is labeled as B (guest chain); the remaining chains are of type A (host). Therefore, we have an extremely dilute solution for B (guest) chains and semidilute solution for host chains.[47]

The lengths of guest and host chains are chosen in our computer experiment as equal to $N_A = N_B = N$ where N was 16, 32, and 64. The interaction energy between nearest-neighbor segments of polymer chains was chosen to be

$$\epsilon_{AA} = \epsilon_{BB} = \epsilon \qquad \epsilon_{AB} = 0 \tag{10}$$

The calculations were made with $\epsilon = 0, 0.06, 0.12, 0.3, 0.42$, and 0.6. This choice of parameters is arbitrary. ϵ was chosen to be "sufficiently bad" in order that the collapse of guest molecules could be observed easily. The attraction between monomers must not be too large, so that Monte Carlo jumps are not inhibited and the algorithm remains effective.[41] The "dynamical" Monte Carlo algorithm with three types of local motions was used: "kink jumps", "90° crankshaft motions", and "end bond reorientations".[38] We employ the classical Metropolis procedure to obtain average values for the quantities of interest.[41] The cube was initially filled by using the biased Rosenbluth–Rosenbluth algorithm.[42] Before start of our "measurement", the system was "well thermalized". This means that the Metropolis procedure for $\epsilon = 0$ was carried out long enough to attain a representative state at high temperatures ($\epsilon = E/kT = 0$). Then we average on 5000 Monte Carlo steps to obtain results for $\epsilon = 0$. Subsequently we use the same system as the initial state for the next smaller temperature ($\epsilon = 0.06$). We thermalized the system at the new temperature, performing 1000 Monte Carlo steps without "measurement" and then "measuring" the average of the next 5000 steps. These procedures are applied to the next smaller temperature ($\epsilon = E/kT = 0.12$), and so on. So it is a kind of "slow cooling" technique that was used because equilibration of dense polymer systems in lattice model simulations is in general a very delicate task.[41] It is especially difficult in the present case, where the collapse of the guest molecule is much more striking than that of the host molecule (see also ref 40). Moreover, because our system for $N = 64$ has only 1 B molecule and at least 86 A molecules (for $N = 32, n = 173$, and for $N = 16, n = 346$), each function for A molecules in one Monte Carlo step was "measured" n times, whereas for the B molecule there was only 1 measurement. This "self-averaging" effect for A molecules leads to much better statistics for the A (host) molecules. Thus one has to be very careful and measure long enough to obtain reasonable statistics for the B molecule, especially for its detailed distribution functions.

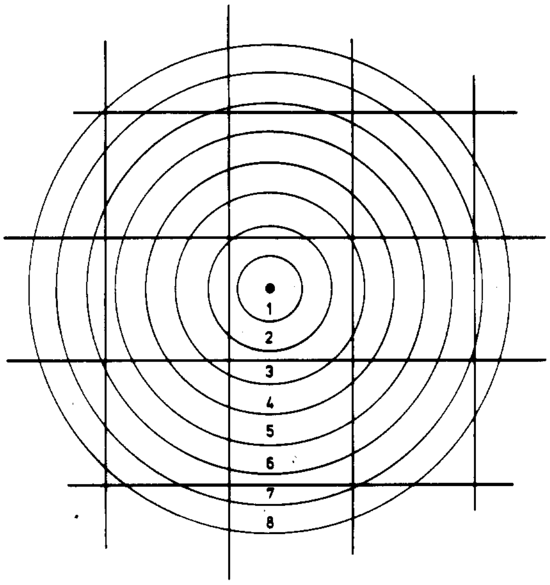

Figure 1. Spherical shells (two-dimensional projection) around the center of inertia of one chain required to calculate the distribution function. The number of shells is depicted.

Therefore we repeated this slow cooling procedure for each N for 10 (or 11 for $N = 64$) independent initial states and finally averaged the results. In our preliminary work on the present topic[40] we only computed the mean-average end-to-end distance and radius of gyration of our model chains. In the present work our main attention will be directed to different density distribution functions with respect to the center of inertia of the molecule. Calculation of the distribution functions was performed in the following way. For each chain, the coordinates of its center of inertia were established in the standard manner:

$$\vec{r}_{CI} = \sum_{i=1}^{N} \frac{\vec{r}_i}{N} \tag{11}$$

(r_i is the coordinate of the ith monomer of the chain.) We then establish the row of $j = 1, 2, 3, ..., k$ spherical shells around the center of inertia of the chain with the radius $r_j = i/4$. ($k = 50$ for $N = 64$; $k = 30$ for $N = 32$; $k = 25$ for $N = 16$.) The 2-dimensional draft of this (3-dimensional) procedure is shown in the Figure 1.

For each space between two adjacent shells $j - 1$ and j we count the whole number of lattice sites found and the number of these sites occupied by A and B monomers. Independently we count the number of monomers belonging to the chain, the center of inertia we just are dealing with. For each host chain we obtain the following density distribution functions:

$$P_{AaA}(r_j) = \frac{\text{number of A monomers}}{\text{number of lattice sites}} \qquad (12)$$

in the space between the $(j-1)$th
and jth spherical shells
around the center of inertia of an A molecule

$$P_A{}^i(r_j) = \frac{\text{number of own monomers of the chain}}{\text{number of lattice sites}} \qquad (13)$$

So $P_{AaA}(j)$ is the density distribution function of host monomers around the center of inertia of host chain. $P_A{}^i(r_j)$ is the density distribution function of monomers of the host chain around its center of inertia.

From these functions it is easy to obtain the "intermolecular" density distribution function of host molecules, i.e., the density distribution function of A monomers, belonging to *another* A chain around the center of inertia of a given A chain.

$$P_{AaA}{}^e(r_j) = P_{AaA}(r_j) - P_A{}^i(r_j) \qquad (14)$$

A similar procedure is used for guest chains. We determine in the same manner the density distribution function of monomers of the A and B type around the center of inertia of the B chain:

$$P_{AaB}(r_j) = \frac{\text{number of A monomers}}{\text{number of lattice sites}} \qquad (15)$$

in the space between the $(j-1)$th and jth
spherical shells around the center of
inertia of a B molecule

$$P_B{}^i(r_j) \equiv P_{BaB}(r_j) = \frac{\text{number of (own) B monomers of the chain}}{\text{number of lattice sites}} \qquad (16)$$

It is obvious that the statistics become essentially better the greater j is, because of self-averaging in the space between large spheres. Then we average arithmetically each distribution function of eqs 12–16 over all chains and all trials and obtain corresponding average functions $\overline{P_{AaA}}(r_j)$, $\overline{P_A{}^i}(r_j)$, etc., which are described below (as a rule we omit j for brevity in the following).

There is one delicate point in our calculation. Namely, the monomers are placed on a lattice but the center of inertia is distributed continuously in space. The distinction between discrete and continuous space displacement causes "coarse-graining" effects. This is particularly striking for small j. In Figure 1 it can be seen that at small j there appear shells not containing any lattice site at all. In this case we would have in all the functions defined by eqs 12–16 the indefinite situation 0/0. Obeying the general rule of Monte Carlo sampling, we count such attempts as "unsuccessful", i.e., as an attempt with the results that all P of eqs 12–16 = 0. It is actually an arbitrary decision (to resolve the uncertainty 0/0 as 0). In general, it is not true. For example, if we suppose that $\overline{P_A{}^{(i)}}(r)$ obeys the Gaussian distribution of eq 3, we know that, as $\overline{P_A{}^{(i)}}(r)$ increases, r (i.e., j) must decrease. In our "computer experiment", however, we obtained a very striking decay of $\overline{P_A{}^{(i)}}(r)$ at very low j, because of the large contribution from "whole" unsuccessful shells without any lattice site at all. However, we think that this effect is only relevant for $r < 1$. Probably it would be reasonable simply to throw away the first three points (j = 1–3) because it is only an artifact of our computer model, which is not chemically realistic on the scale of the lattice spacing, but we keep these points at least for the presentation of our "raw results" to display fully the data that have been obtained.

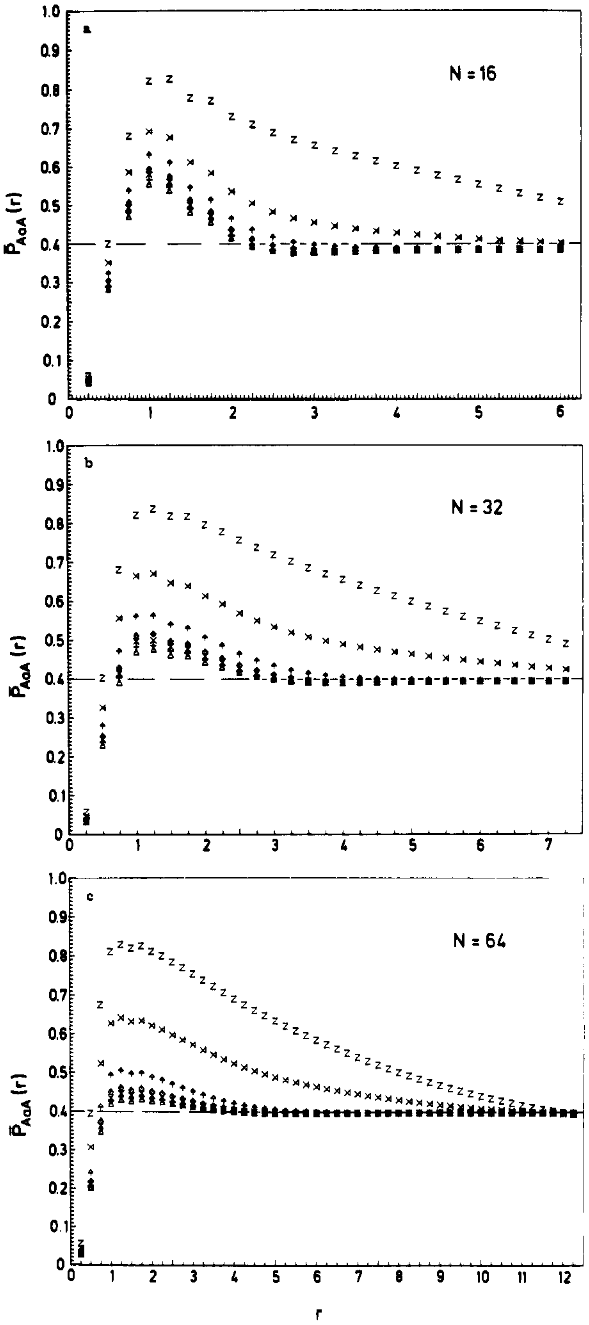

Figure 2. Density distribution function of monomers of the host type around the center of gravity of one host chain for different N (a–c) and ϵ (Table I). The broken line indicates the polymer concentration in the system.

3. General Structure of Semidilute Solution

Figure 2 shows the distribution function of monomers in a host chain, around the center of gravity of one host chain, $\overline{P_{AaA}}(r)$. Parts a–c of Figure 2 show the results for different N, and for each N several solvent qualities are indicated. At $r = 1$ we observe a maximum in the $\overline{P_{AaA}}(r)$ function. This maximum increases with the average density of the polymer in the solution. With increasing r the mean local density decays and reaches the mean-average density of the polymer solution ($c = 0.4$).

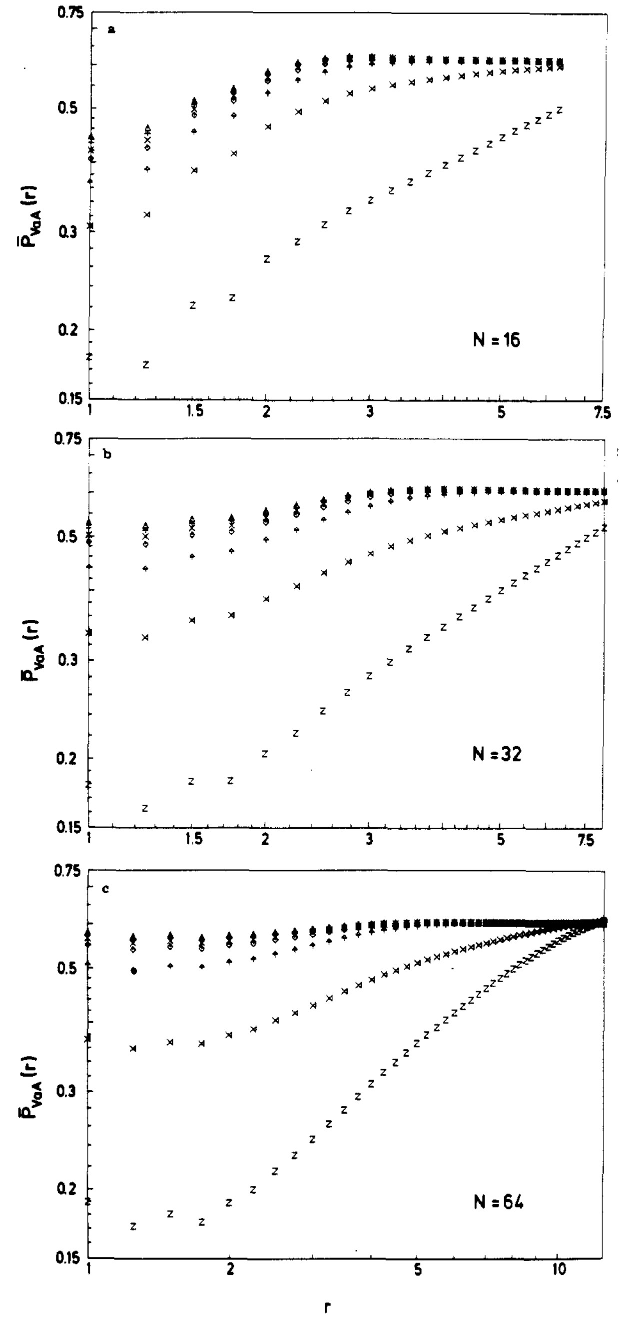

Figure 3. log–log plot of the density distribution of vacancies around the center of inertia of one host molecule for different N (a–c) and ϵ (Table I).

The question arises whether this behavior is an effect reflecting the equilibrium structure of one phase consisting of polymer and solvent or whether the tendency of phase separation between polymer and solvent is here indicated (at least slightly). When ϵ increases, we finally have to achieve the condition where the polymer–low molecular weight solvent system separates into two phases—one phase rich in polymer and another rich in solvent. This topic was not studied in our previous work,[38-40] and we are not aware of other papers where polymer-vacancy phase separation in similar model systems is studied. Therefore, we do not know the exact value of the parameter ϵ for which phase separation can be expected in the chain-vacancy system on the (cubic) lattice. However, there are older studies[43,44] performed on a similar cubic lattice model for an isolated chain, where it was shown that the Θ-condition for a chain in this model occurs at $\epsilon \approx 0.3$. This means that we can expect polymer–solvent phase separation for sufficiently large N in the vicinity of 0.3.

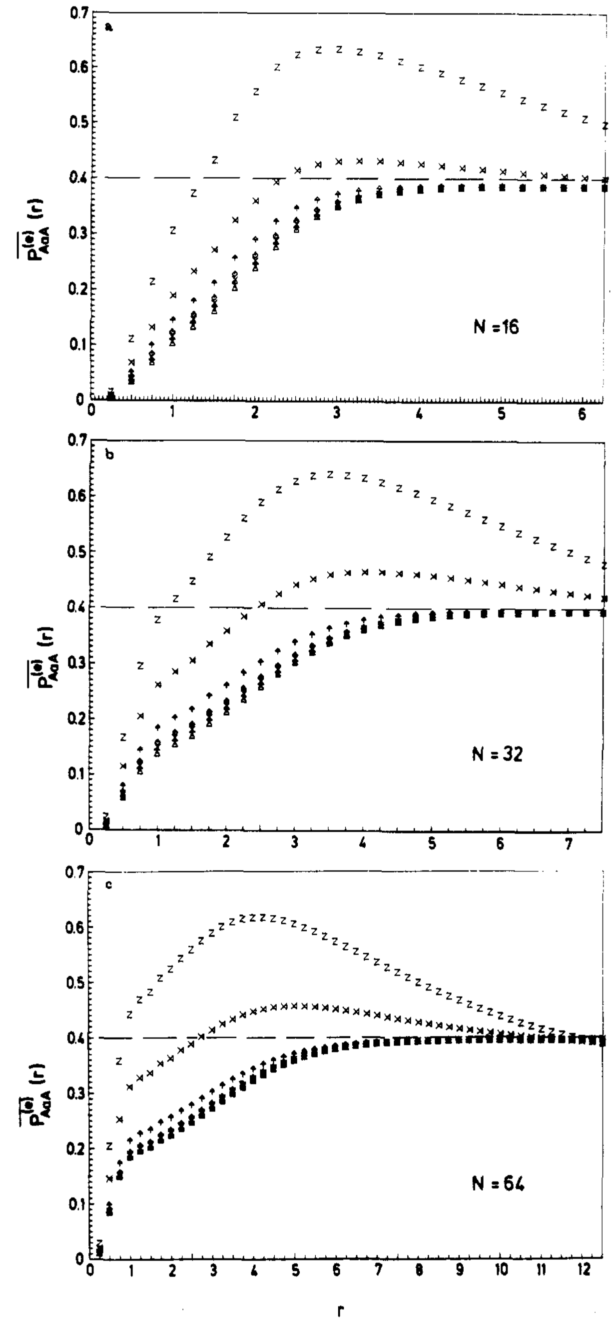

Figure 4. Density distribution of host monomers, belonging to other chains, around the center of gravity of a given host chain for different N (a–c) and ϵ (Table I). The broken line indicates the polymer concentration in the system.

To make a better judgement (at least, qualitatively) of what we have to expect in our chosen situation, we show in Figure 3 the vacancy distribution functions around the center of inertia of polymer chain $\overline{P}_{vaA}(r)$ ($\overline{P}_{vaA}(r) = 1 - \overline{P}_{AaA}(r)$) in a log–log presentation. In Figure 3 we can clearly see two tendencies already indicated in Figure 2 but much more obvious in Figure 3. First of all, we see that for a certain ϵ interval (ϵ = 0–0.18) the "lack of vacancies" (locally vacancy concentration $c_v(r) < 0.6$) is a relatively "short range" effect, observed until $r = 2.5$. This short-range effect is seen more clearly for $\epsilon = 0$ where, in an athermal solution, we are sure to have strictly one phase.

Another tendency is observed clearly for ϵ = 0.42 and 0.6. Here the lack of vacancies is much more pronounced and tends to spread. This effect seems to be connected with the tendency to macroscopical polymer–solvent phase

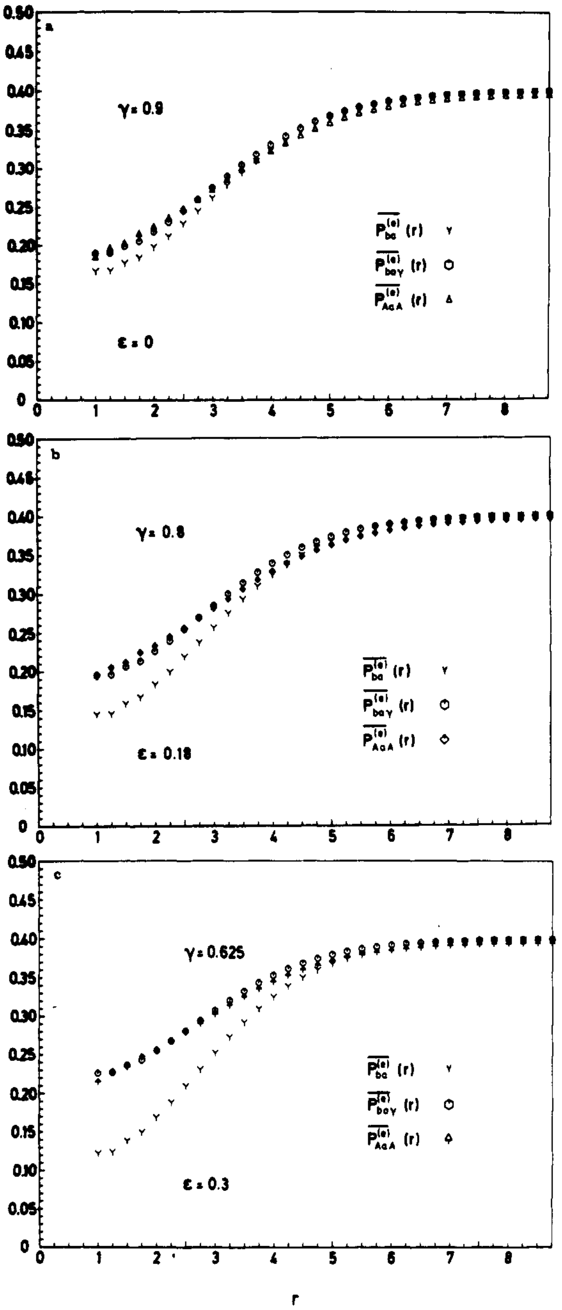

Figure 5. Fitting of "computer experiment results" for $\overline{P_{AaA}^{(e)}(r)}$ (from Figure 4) (for ε drawn from the figures, $N = 64$) with "quasi-binary ansatz" (eq 18) and "improved quasi-binary ansatz" (eq 19) (γ, drawn on the figures).

separation (at least, as a "pretransitional effect"). This effect is seen better for larger N, in agreement with the general ideas on polymer–solvent phase transitions.[22] We return to the interesting topic regarding "average density structure" in a strictly one-phase polymer–solution system in the general discussion at the end of this paper. At this point it is only important to notice that we seem to achieve two thermodynamic regions in our calculation: the region where a strictly one-phase polymer–solvent system exists and a region that shows a tendency toward polymer–solvent separation.

4. "Correlation Hole" for Semidilute Solution

Figure 4 shows the mean-average density of monomers belonging to other chains around the center of gravity of a chosen chain for semidilute (host) solution $\overline{P_{AaA}^{e}(r)}$.

It is qualitatively similar to the "correlation hole" well-defined for polymer melts.[22] At small r we see the trivial gap or "screening"; i.e., penetration of the monomers of other chains becomes increasingly difficult the shorter the distance from the center of inertia of a given chain because the space is filled by the monomers of this given chain.

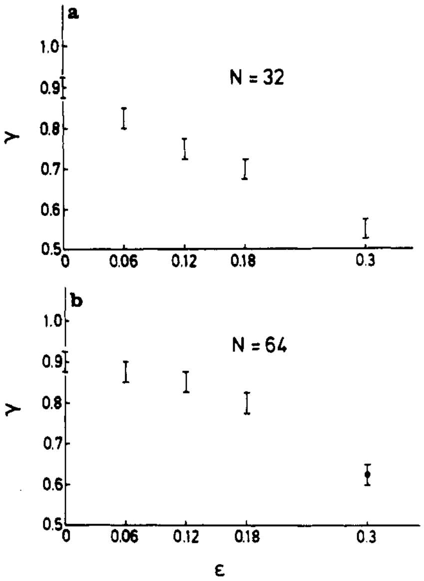

Figure 6. Fit of parameter γ of eq 19 versus ε for $N = 32$ (a) and 64 (b).

We see that for $\epsilon = 0.42$ and 0.6 for "intermediate" r $\overline{P_{AaA}^{e}(r)}$ is larger than the mean density of the polymer solution, which is 0.4, reflecting the tendency of aggregation of molecules in a cluster by polymer–solvent separation. For the "one-phase case" $\epsilon = 0$–0.3, $\overline{P_{AaA}^{e}(r)}$ is enhanced monotonically until it reaches the mean polymer concentration. We tried to apply different scaling assumptions to check the possible "universalities" in our correlation hole at least for the one-phase case ($\epsilon = 0$–0.3), but we were not successful. The only reasonable chance of obtaining a qualitative picture of the behavior of the correlation hole in our "one-phase region" ($\epsilon = 0$–0.3) is to compare our results with a simple "quasi-binary" assumption:

$$\overline{P_A^{(i)}(r)} + \overline{P_{AaA}^{(e)}(r)} = c \tag{17}$$

The means that the mean concentration of the polymer, c (0.4 in our case), must be the sum of the monomers belonging to the given chain and monomers belonging to other chains on each site. From Figure 2 we see it is not strictly true even for $\epsilon = 0$, where $\overline{P_{AaA}(r)}$ for r between 1 and 2 is distinctly larger than 0.4. This fact reflects the importance of density fluctuations on the local length scale in both melts and solutions.[27] The question arises whether it is possible to capture some general features of this effect using quasi-binary ansatz. We actually succeed when we replace the quasi-binary ansatz

$$\overline{P_{ba}^{(e)}(r)} = 0.4 - \overline{P_A^{(i)}(r)} \tag{18}$$

by

$$\overline{P_{ba\gamma}^{(e)}(r)} = 0.4 - \gamma\cdot\overline{P_A^{(i)}(r)} \tag{19}$$

where γ is a fit parameter.

Figure 5 shows some examples where the "experimental" $\overline{P_{AaA}^{e}(r)}$ was fitted by using eqs 18 and 19.

The fit for $\overline{P_{ba}^{(e)}(r)}$ using eq 18 is not successful even for $\epsilon = 0$, but the fit for $\overline{P_{ba\gamma}^{(e)}(r)}$ using an appropriate γ is

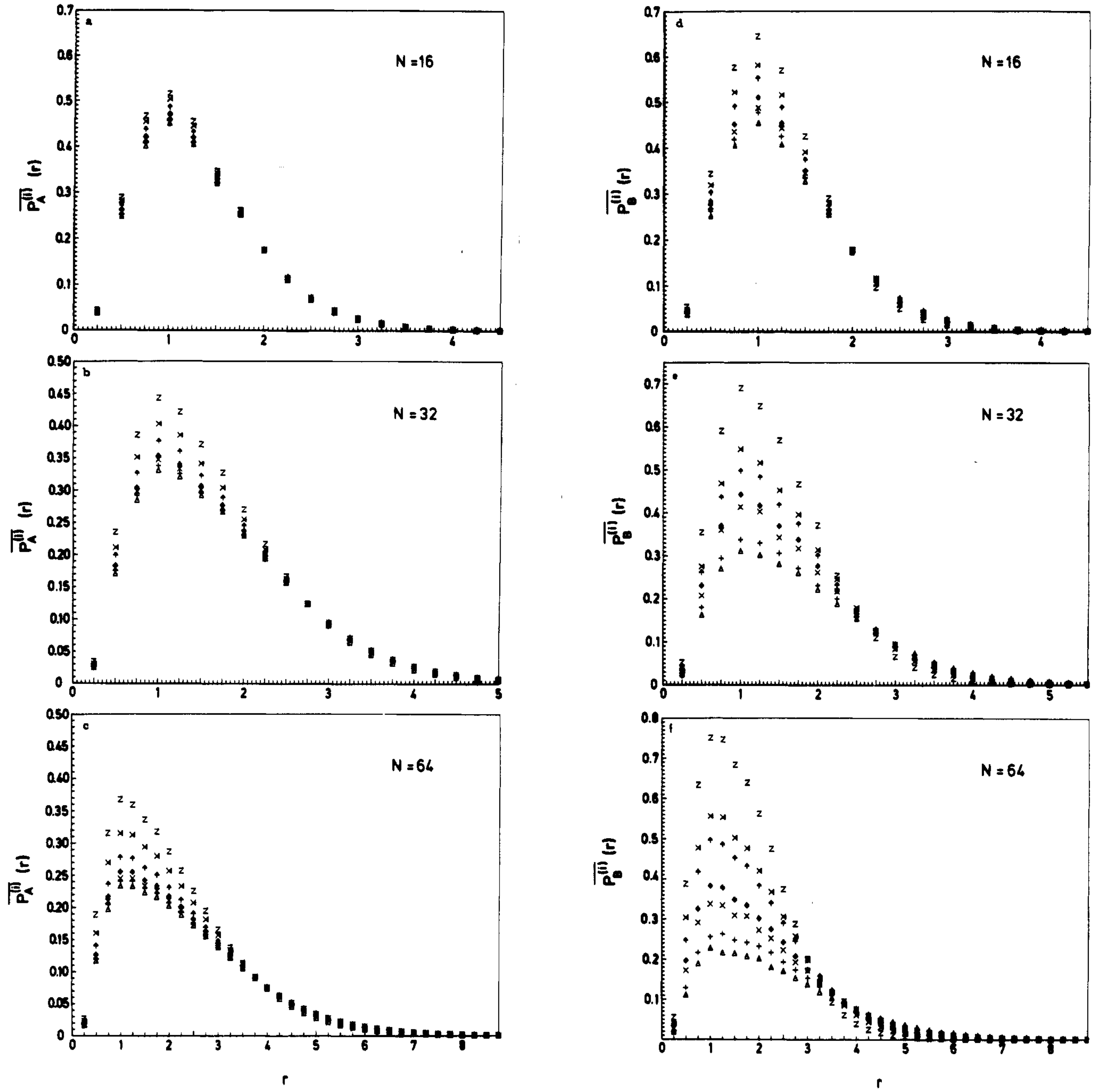

Figure 7. Density distribution function of monomers of host chain (a–c) and guest chain (d–f) around its own center of inertia for different N and ϵ (Table I).

astonishingly good. Using this procedure, we find one "empirical" parameter γ for each N and ϵ. In Figure 6 $\gamma(\epsilon)$ is shown for N = 32 and N = 64.

This fitting procedure has the following physical sense: the monomers of other chains fill more space around a given chain in comparison with the quasi-binary prediction $c(r)$ = 0.4, and this "overfilling" happens in a specific manner. Namely, this overfilling is proportional to the density of a given chain for each r, with a proportionality coefficient γ depending only on ϵ (and N but not on r(!)). This means that the overfilling depends primarily on the energy of interaction between monomers of a given chain and the surrounding chains, which is obviously proportional to the density of monomers of the given chain on each site.

So, vice versa, if we try to describe this effect in the language of the quasi-binary approximation we show that the effective density "shrinks" by a factor γ, depending on ϵ. So the overfilling effect seems to be mainly of energetic origin. Nevertheless, the fact that for ϵ = 0 it is possible to achieve a visibly better fit of $P_{\mathrm{AaA}}{}^{(\mathrm{e})}(r)$ with $P_{\mathrm{ba}\gamma}{}^{(\mathrm{e})}$ by using γ = 0.9 (and not by the true quasi-binary approximation γ = 1) shows that the "conformational" or entropic contribution plays some role in these overfilling effects too.

From Figure 2 we see that this overfilling effect for the one-phase region loses its importance for large N, where we expect only a small correction if it does not disappear altogether.

But it is unknown whether such effects play any role in real polymer systems and to investigate it would be an interesting task.

Nevertheless, the amazing fact that with formula 19 it is possible to fit the correlation hole very well appears to be sufficiently interesting to describe it explicitly as has been done here.

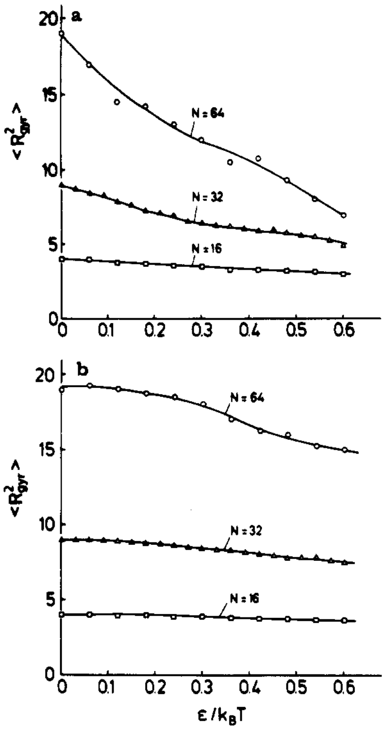

Figure 8. Mean-square radius of gyration, $\langle R_g^2 \rangle$ (in units of lattice constant), plotted versus inverse temperature as expressed by the dimensionless ratio of interaction energy and absolute temperature $\epsilon / k_B T$ for the guest chain (a) and host chain (b).

5. Shape of the Guest and Host Molecules

In Figure 7 we see the density distribution function for monomers of one chain around the center of gravity for host and for guest chains. To make the following discussion more illuminating, we show in Figure 8 the curve from ref 40, where the radius of gyration for host and guest chains is given versus ϵ. From Figure 8, we see that the guest polymer collapses much more than the host polymer. This is clear from the results of Figure 7, too. Namely, the shape of the guest molecule with increasing ϵ becomes much narrower and its maximum increases more than for the host polymer. In principle, the density distribution functions are very appropriate in order to check a "blob concept", especially the thermal-blob concept describing the way in which the guest molecule shrinks with increasing strength of interaction. To pursue this task, however, it is necessary to perform similar calculations at least for different host concentrations and probably for larger N.

Moreover, the relevant characteristics for this purpose were the distribution functions around the chosen monomer of the chain and not around its center of gravity. So we are here interested only in general features of the shape of the host and guest molecules.

The requirements of normalization for one molecule suggest a universal law of the type[22]

$$P^{(i)}(r) = \frac{N}{R_g^3} f\left(\frac{r}{R_g}\right) \tag{20}$$

This type of scaling is actually fulfilled nicely.

Figure 9 shows the data of Figure 7 replotted in relevant coordinates with R_g depicted from Figure 8. If we do not pay attention to the ambiguous points on small r/R_g (corresponding to $r < 1$), we see that all seven curves for each case obey the universal scaling law. Moreover, this law is universal for all six subfigures (also for guest as well as for host molecules), and the scaling function has a simple Gaussian form!

Thus, our results obey the simple law

$$\frac{R_g^3}{N} \overline{P^{(i)}}\left(\frac{r}{R_g}\right) = \alpha \exp\left(-\frac{3}{2} \frac{r^2}{R_g^2}\right) \tag{21}$$

and the best fit coefficient α turns out to be nearly $\alpha \sim 0.37$ (this value lies in the vicinity of the "classical"[21] normalization coefficient $(3/2\pi)^{3/2} = 0.33$ for a Gaussian distribution from (eq 3)).

The universal law $P^{(i)}(r) \sim (1/R_g^3)\phi(r/R_g)$ is obviously the same as the universal law of Des Clouseaux, $P(r) \sim (1/R_g^3)\phi(rN^{-\nu})$, in the asymptotic region because $R_g \sim N^\nu$ for large N. But "our" law is "much more universal", because it is true for different crossover situations between different "solvent goodness" regions and for moderate N.

6. Host Monomer Environment around the Guest Molecule

Finally, we show in Figure 10 the monomer distribution of host molecules around the center of gravity of the guest macromolecule. From this figure it is possible to obtain information about the structure of mixed (polymer A–low molecular weight) solvent around the very dilute macromolecule B. The energetic conditions chosen in the present work ($\epsilon_{AA} = \epsilon_{BB}$, $\epsilon_{AB} = 0$) imply that in contrast to Figure 4 the interpenetration of host monomers into the guest molecule increases as ϵ decreases. Actually, we can demonstrate different phase situations in this plot. (a) Guest, host, and vacancies form one phase. (b) Guest and host molecules are incompatible and build two thermodynamic phases: guest–vacancy phase and host–vacancy phase. This means that the guest molecule is surrounded by a cloud of vacancies, and the presence of host monomers in the vicinity of the guest molecule is very unwelcome. There appears a very interesting separate question about the shape of the phase boundary between host–vacancies and guest–vacancies phases. (c) The phase separation between host polymer and vacancies is possible (see section 3).

In refs 38 and 39 we studied explicitly the conditions for phase separation between two polymer species in a common good solvent for the present lattice model. We reached quite low concentrations of one polymer species there, and it enabled us to obtain information about the phase conditions relevant for "B" (see especially Figure 6a of ref 39).

This analysis is restricted because in the region of small concentration of one species the phase diagram is extremely nonlinear; therefore, to extrapolate the phase diagram for a small concentration of one species to "0" concentration is quite a cumbersome task. Nevertheless, this result allowed us to judge that for $N = 16$ and probably for $N = 32$ we are in the one-phase region for polymer–polymer phase separation (polymer–polymer phase separation (if it occurs at all) begins then only for $\epsilon > 0.3$). But for $N = 64$ we probably have to expect visible polymer–polymer phase separation.

In Figure 11 we replot Figure 10 using a different normalization of the abscissa, namely

$$x = \frac{R_{gB}^2}{N} \equiv \frac{R_{gB}^3}{N} \frac{r}{R_{gB}} \sim \frac{1}{\rho_B} \frac{r}{R_{gB}}$$

where $\rho_B = N/(4/3)\pi R_{gB}^3$ is the mean intramolecular density of B monomers and R_{gB} seems to be the "natural" measure of length that scales spatial variation around a B molecule). From Figure 11 we see that for $N = 16$ and $N = 32$ there are two ϵ regions. In one region ($\epsilon = 0$–0.3) we nearly have universality in these "scaled" coordinates.

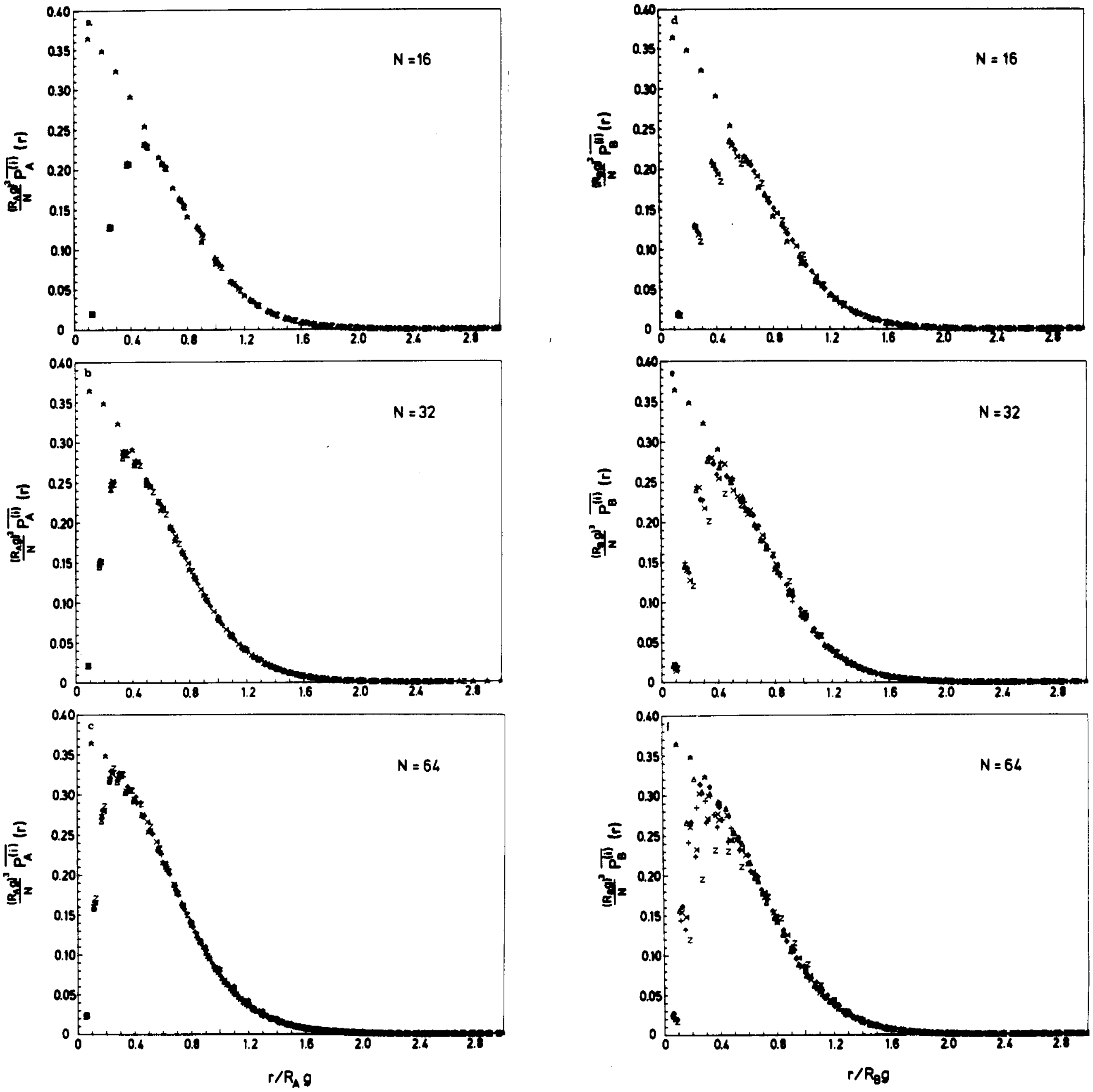

Figure 9. Density distribution function of monomers of host chain (a–c) and guest (d–f) chain (data of Figure 7) replotted in appropriate scaling coordinates (eq 20) with radius of gyration R_g from Figure 8 for different N and ϵ (from Table I). ★ points obtained from eq 21 with α = 0.37.

The curves for $\epsilon = 0.42$ and 0.6, however, do not obey this universal law. On the other hand, our supposition about universality in N is obviously not valid at all (the slopes of the curves for different N deviate).

We interpret this picture with the following hypothesis. The law of the type

$$\overline{P_{\mathrm{AaB}}}(r) = F(r\cdot R_g^{\,2}) \qquad (22)$$

actually holds for the strictly one-phase region where neither polymer–polymer phase separation nor polymer–vacancy phase separation occurs. This seems to be a consequence of the fact that we do not have energetic interactions between guest and host molecules ($\epsilon_{\mathrm{AB}} = 0$). So the guest molecule builds only geometrical obstacles for the host monomers, but the guest molecule obeys the scaling law of eq 20. So, the host monomers, following the shape of the guest molecule in the vicinity of its center of gravity, follow a similar law, but if any kind of supplementary circumstances appear (any kind of phase separation or "preseparation" conditions), the situation is no longer controlled by geometrical effects only and becomes more complicated. Therefore, it is impossible to describe it by using the simple law. We assumed that the deviation of the curves in Figure 11 for $\epsilon = 0.42$ and $\epsilon = 0.6$ from the "universal" behavior for $N = 16$ and 32 is the result of host monomer phase separation and that the "confusion" for $N = 64$ is the result of complicated interplay between guest–host and host–vacancy phase separation. This statement is not very serious; it is only needed to make the picture drawn in this paper "self-consistent". In general, much more work is necessary to fully clarify this fascinating topic.

7. Conclusions

For the first time the density distribution functions for ternary polymer–polymer–solvent systems were obtained

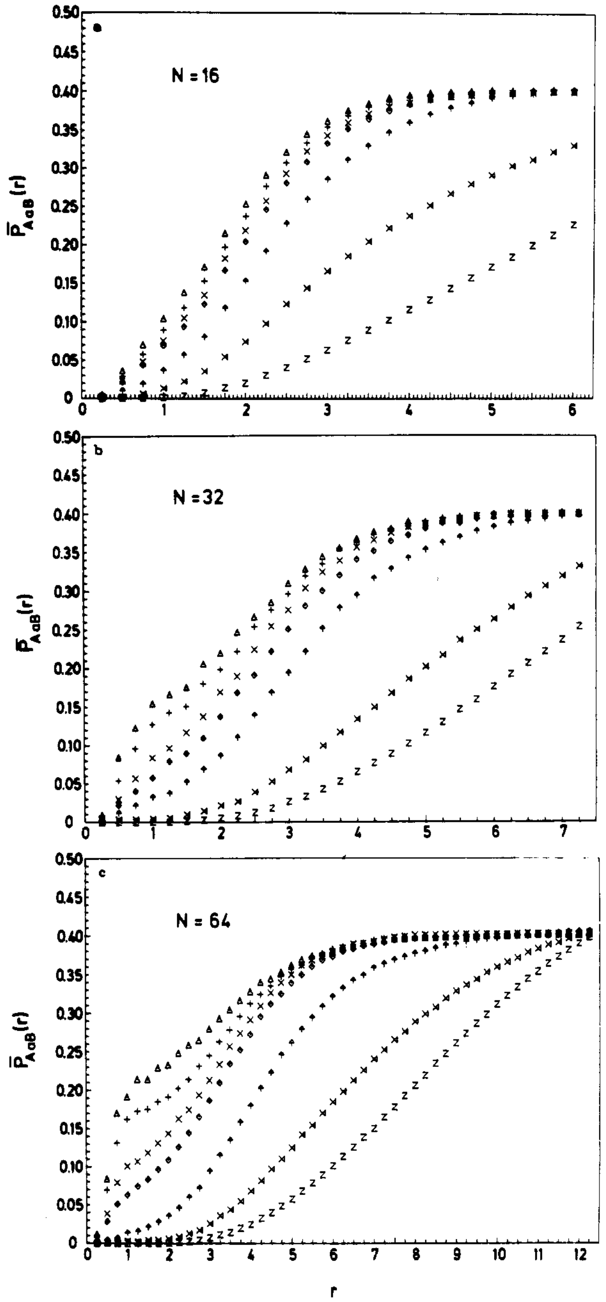

Figure 10. Density distribution function of the host monomers around the center of inertia of the guest chain for different N and ϵ (Table I).

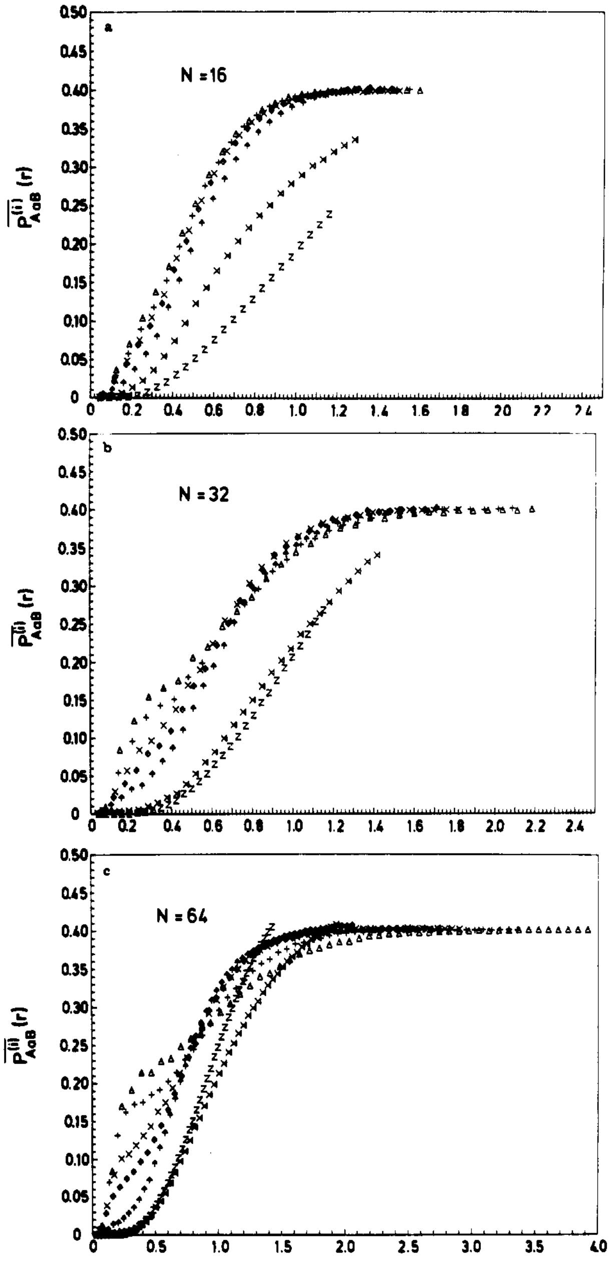

Figure 11. Data of Figure 10 replotted in appropriate "scaled" x coordinates (eq 22).

in model computer calculations. We choose the "extreme" case: only one molecule of one species (B, guest molecule) was put into the binary system, consisting of 40% of polymer A (host polymer) and 60% vacancies (low molecular weight solvent). It would be desirable to model ternary systems with other polymer A–polymer B concentrations, but the calculation of distribution functions is quite expensive in computer time. Therefore, we restricted attention to the present most striking case. This case is of special interest in connection with the "coil–globule transition", and here this transition occurs in a mixed solvent consisting of another polymer and low molecular weight fluid. We were not able to study in this work the asymptotic behavior of the coil–globule transition in order to decide whether it is a phase transition of II or I order or otherwise. We studied only the general behavior of the shape of the B molecule and the manner in which the host monomers interpenetrate in this single molecule. Another interesting task was the monomer distribution behavior of semidilute (A) chains in low molecular weight solution.

(1) Our first surprisingly simple result is the Gaussian-like behavior of the shape of A as well as of B molecules (eq 21), despite the great differences in A- and B-chain behavior. (2) Another result (Figure 11) is that in the "strictly one-phase situation" the interpenetration of A monomers in the B molecule obeys the scaling law. This result could be connected with our choice of parameters ($\epsilon_{AB} = 0$). In this situation B chains only build geometrical obstacles for A monomers, not affected by preference due to energetic interactions. (3) The most interesting topic in our study seems to us to be the question regarding polymer–solvent separation. We observed at $\epsilon = 0.42$ and 0.6 visible separation between A monomers and vacancies for the "whole length of observation", i.e., all distance intervals. The pair correlation functions were measured, but whether this effect is an indication for incipient phase separation (of first order?[22]), a kind of "pretransitional effect", is not clear and requires much more work. (4) In

the strictly homogeneous (or one-phase) situation (Figure 2, $\epsilon = 0$–0.3) the polymer density in the vicinity of the center of inertia of a given chain is on average a little higher than the mean concentration of the polymer in solution. It is an open question whether this effect appears only for the moderate chain lengths modeled in our system (rule of thumb is that each link of our chain model is approximately 1 statistical segment of a real polymer—our chains thus model oligomers with a molecular mass of a 10 000 and more) or if this (slight) effect has general significance. It depends on the manner in which monomers of other chains interpenetrate with the given chain or, in other words, on how one molecule screens the space where it is situated. We did not find any plausible ideas about this topic in the literature, and so we restricted ourselves to purely empirical trials in order to describe this effect in an "improved quasi-binary approximation" (see section 4). We consider this modest attempt only as a motivation for more serious work in this direction.

In our simulation of the spinodal decomposition of a similar model,[45] where we quenched the polymer A–polymer B–solvent from $\epsilon = 0$ to large ϵ (low temperatures), we observed that there is one striking effect after quenching at the beginning of spinodal decomposition: namely, the macromolecules shrink. This effect actually "correlates" very well with the effect of enhanced density concentration in the vicinity of the center of gravity of the molecule. Namely, the separation between A and B species in spinodal decomposition has to occur with a "negative diffusion coefficient", i.e., in the opposite direction to the density gradient.[46] We observe in Figure 2 a slight density gradient, which should "invite" other monomers to follow this direction during quenching, and so the macromolecule shrinks. One can imagine other interesting phenomena related to this "enhanced density effect". For example, it is plausible that it could facilitate the building up of an initial cluster for nucleation of the new phase in the "metastable" region.

Acknowledgment. I thank the Max Planck Institut für Polymerforschung, Mainz, for financial support. I am very indebted to K. Binder, H. L. Frisch, J. F. Joanny, and E. B. Zhulina for stimulating discussions. Particular thanks are due to K. Binder for critical reading of the manuscript.

References and Notes

(1) Volkenstein, M. V. *Molecular Biophysics*; Nauka: Moscow, 1975.
(2) Williams, C.; Brochard, F.; Frisch, H. L. *Annu. Rev. Phys. Chem.* **1981**, *32*, 433.
(3) Chu, B.; Park, I. H.; Wang, S. W.; Wu, C. *Macromolecules* **1987**, *20*, 2833. Chu, B.; Xu, R.; Zuo, J. *Macromolecules* **1988**, *21*, 273.
(4) de Gennes, P.-G. *J. Phys. Lett.* **1975**, *36*, L-55.
(5) Moore, M. A. *J. Phys. A: Math. Gen.* **1977**, *10*, 305.
(6) Lifshitz, I. M.; Grosberg, A. Yu.; Khochlov, A. *Rev. Mod. Phys.* **1978**, *50*, 683.
(7) Post, C. B.; Zimm, B. H. *Biopolymers* **1979**, *18*, 1487.
(8) Elyashevich, A. M.; Skvortsov, A. M. *Mol. Biol. USSR* **1971**, *5*, 204.
(9) Daoud, M.; Jannink, C. *J. Phys. (Paris)* **1978**, *39*, 33.
(10) Lerman, L. S. *Proc. Natl. Acad. Sci. U.S.A.* **1971**, *68*, 1886.
(11) Frisch, H. L.; Fesciyan, S. *J. Polym. Sci., Polym. Lett. Ed.* **1979**, *17*, 309.
(12) Tanaka, F. *J. Chem. Phys.* **1983**, *78*, 2788; **1985**, *82*, 2466.
(13) Tanaka, F.; Ushiki, H. *Macromolecules* **1988**, *21*, 1041.
(14) Ushiki, H.; Tanaka, F. *Eur. Polym. J.* **1985**, *21*, 701.
(15) Nose, T. *J. Phys. (Paris)* **1986**, *47*, 517.
(16) Joanny, J. F.; Grant, P.; Pincus, P.; Turkerich, L. A. *J. Phys. (Paris)* **1981**, *42*, 1045; *J. Appl. Phys.* **1981**, *52*, 5943.
(17) Kuhn, R.; Cantow, H. J. *Macromol. Chem.* **1969**, *122*, 65.
(18) Lin, C. Y.; Rosen, S. L. *J. Polym. Sci.* **1982**, *20*, 1497.
(19) Cotts, D. R. *J. Polym. Sci., Polym. Phys. Ed.* **1983**, *21*, 1381.
(20) Humasawa, N.; Hamada, T.; Nose, T. *J. Polym. Sci., Polym. Lett. Ed.* **1985**, *23*, 1.
(21) Flory, P. J. *Statistical Mechanics of Chain Molecules*; Wiley-Interscience: New York, 1969.
(22) de Gennes, P.-G. *Scaling Concepts in Polymer Physics*; Cornell University Press: Ithaca, NY, 1979.
(23) Des Cloizeaux, J. *J. Phys. (Paris)* **1980**, *41*, 22.
(24) Chang, L. P.; Morawetz, H. *Macromolecules* **1987**, *20*, 428.
(25) Fridrickson, G. H. *Macromolecules* **1986**, *19*, 44.
(26) Curro, J. G.; Schweizer, K. S. *J. Chem. Phys.* **1987**, *87*, 1842.
(27) Curro, J. G.; Schweizer, K. S. *Macromolecules* **1987**, *20*, 1928.
(28) Schweizer, K. S.; Curro, J. G. *Macromolecules* **1988**, *21*, 3070.
(29) Bluestone, S.; Vold, M. J. *J. Polym. Sci., Part A: Gen. Pap.* **1964**, *2*, 289.
(30) Wall, F.; Seitz, W. A. *J. Chem. Phys.* **1977**, *67*, 3722.
(31) Okamoto, H. *J. Chem. Phys.* **1979**, *70*, 1690.
(32) Birshtein, T. M.; Skvortsov, A. M.; Sariban, A. A. *Polymer* **1983**, *24*, 1145.
(33) Kolinski, A.; Skolnick, J.; Jaris, R. *J. Chem. Phys.* **1987**, *86*, 1567.
(34) Olaj, O. F.; Pelinka, K. H. *Macromol. Chem.* **1976**, *177*, 3413.
(35) Vacatello, M.; Avitabile, G.; Corradini, P.; Tuzi, A. *J. Chem. Phys.* **1980**, *73*, 548.
(36) Kremer, K.; Baumgärtner, A.; Binder, K. *J. Phys. A: Math. Gen.* **1981**, *15*, 2879.
(37) Bishop, M.; Ceperley, D.; Frisch, H. L.; Kalos, M. H. *J. Chem. Phys.* **1980**, *72*, 3228.
(38) Sariban, A.; Binder, K. *J. Chem. Phys.* **1987**, *86*, 5859.
(39) Sariban, A.; Binder, K. *Macromolecules* **1988**, *21*, 711.
(40) Sariban, A.; Binder, K. *Macromol. Chem.* **1988**, *189*, 2357.
(41) Binder, K., Ed. *Monte Carlo Method in Statistical Physics*; Springer: New York, 1979.
(42) Rosenbluth, N. M.; Rosenbluth, A. W. *J. Chem. Phys.* **1959**, *23*, 356.
(43) Mazur, J.; McCrackin, F. *J. Chem. Phys.* **1968**, *49*, 648.
(44) Birshtein, T. M.; Skvortsov, A. M.; Sariban, A. A. *Macromolecules* **1977**, *10*, 202.
(45) Sariban, A.; Binder, K. *Polym. Commun.* **1989**, *30*, 205.
(46) Gunton, J. D.; San Miguel, M.; Sahni, P. S. In *Phase Transitions and Critical Phenomena*; Domb, D., Lebowitz, J. L., Eds.; Academic Press: London, 1983; Vol. 8, p 267.
(47) The value of $c^* \approx N/(4/3)\pi R_g^3$ determining the concentration of overlapping of polymer coils in solution may be estimated from the data of Figure 8. At $N = 16$, 32, and 64 and $\epsilon = 0$, one obtains $c^* = 0.47$, 0.28, and 0.18. Hence, at least for the values of $N = 32$ and 64 our system is under the conditions of a semidilute solution ($c^* < c = 0.4$), and for $N = 16$ we are in the crossover region between a dilute and a semidilute solution.